University of Birjand

Water Harvesting Research (2025) Vol. 8, No. 2: 299-309

10.22077/jwhr.2026.10501.1192

ORIGINAL ARTICLE

Investigation of Sand Trap and Bar Screen Mechanisms on Urban Drains (Case Study: Shahjalal Upashahar, Sylhet, Bangladesh)

Ashutus Singha[a*], Rabia Sultana[a], Sumiya Akter[a], A. K. Mohibul Islam[a]

[a]Department of Irrigation and Water Management, Sylhet Agricultural University, Sylhet-3100, Bangladesh.

[*]Corresponding Author E-mail address: ashutus.iwm@sau.ac.bd

Received: 16 November 2025, **Revised**: 20 December 2025, **Accepted**: 25 December 2025

Abstract

Improper maintenance, inadequate drainage system design, and increasing non-porous surfaces due to urbanization result in waterlogging in urban areas. Shahjalal Upashahar is a prominent urban area in Sylhet city which faces waterlogging conditions due to sediment deposition, leading to the loss of original drainage channel capacity. This study focused on reducing the sediment accumulation in the drainage channel by implementing a sand trap and bar screen mechanism. To design the sand trap for a 100-year return period, the study area was divided into five sub-watersheds using the ArcGIS tool. Rainfall data (2000-2023) were collected from the nearby meteorological station. Based on the determined slope and length of all sub-catchments, the concentration times range from 10.995 to 13.8707 minutes. Using the concentration time, the rainfall intensity was calculated from the Intensity Duration Frequency curve (IDF). The highest runoff was calculated for all sub-watersheds using the rational equation. The peak discharge for catchments 1 through 5 were 1.263, 1.784, 0.254, 1.183 and 1.326 m^3/sec, respectively. The required cross-section of the rectangular sand trap was determined using the equation of continuity Q = AV. The bar screen was designed based on the size of solid waste and the prevailing velocity of flow. In this study, the designed cross-sectional areas of sand traps ranging from 0.38 to 2.26 m^2 for five sub-watersheds were expected to reduce sediment accumulation by maintaining full drainage channel capacity.

Keywords: IDF curve, Rational equation, Sedimentation, Time of concentration, Waterlogging.

1. Introduction

As global changes such as urbanization and climate change intensify, future cities will face challenges in managing water supply, drainage, and wastewater (Vairavamoorthy et al., 2008). To manage stormwater and wastewater of urban areas and convey them away from those areas, urban drainage system plays significant role (Chocat et al., 2007; Thodesen et al., 2022).

Flood risk rises in cities due to local changes in hydrological and hydro-meteorological conditions as well as Urban development i.e., increased urban runoff driven by imperviousness (Huong & Pathirana, 2013; Lu et al., 2025). High amount of runoff causes sediment accumulation result in reduction of actual capacity of drainage (Addison-Atkinson et al., 2024; Dibaba, 2018).

In Bangladesh, rapid population growth has accelerated urbanization nationwide. Sylhet City Corporation (SCC), a metropolitan area in northeastern Bangladesh, often experiences urban flooding and waterlogging from storm runoff during heavy rains. The city struggles with severe drainage congestion, stemming from an inadequate drainage system, poor maintenance, garbage disposal in drains and canals, and illegal encroachment on drainage canals (Islam and Rahman, 2022). The city also experiences sediment accumulation and solid waste disposal in its drainage system (Azir, 2025).

In Sylhet, the monsoon season typically runs from May to September, characterized by hot, humid conditions and frequent heavy rains, while the brief dry season lasts from late October to February, with hot and relatively clear weather (Ahmed and Kim, 2003). Nearly 80% of the annual average rainfall of 3334 mm occurs in this region between May and September (Choudhury et al., 2012).

This area is situated within a region of hills and basins, one of the most distinct areas in Bangladesh. Northeastern Bangladesh is also highly vulnerable to environmental hazards like waterlogging (Sarker and Rashid, 2013).

Sylhet City Corporation is grappling with severe waterlogging issues. The annual monsoon season brings persistent waterlogging that inundates homes, farmlands, ponds, streets, orchards, and grasslands, among other areas (Hossain et al., 2022; Roy et al., 2022). Intense rainfall and upstream water flow have led to widespread flooding in Sylhet, affecting around 1.6 million people, with nearly 30,000 seeking refuge in shelters. The Surma and Kushiyara rivers overflowed, submerging large parts of the city and its surrounding district.

According to The Daily Star (2024), Continuous rainfall has caused flooding to recur, submerging areas, and over 16,000 people have been relocated to shelters as the rivers continue to rise. Disposal of solid waste in drainage paths reduces the drainage system's capacity, leading to unwanted waterlogging during heavy rains.

Waterlogging due to drainage congestion contaminates groundwater, posing a public health risk if cities use this groundwater or polluted surface water for domestic purposes (Phanuwan et al., 2006; Ten Veldhuis and Clemens, 2010). There are so many approach to calculate the runoff discharge, such as: SCS or NRCS curve number (CN) method (Cronshey, 1986), Unit Hydrograph method, Green- Ampt method, Hydrologic Routing method, Variable Infiltration Capacity (VIC) etc. (dos Santos et al., 2023; Gowdish & Muñoz-Carpena, 2009; Jain et al., 2025; Miller, 1984).

The rational approach, a commonly used method because of its simplicity and minimal data requirement as well as to determine runoff discharge of small watersheds (Hua et al., 2003). The Intensity-Duration-Frequency (IDF) curve is used in this method. It offers valuable insights into rainfall patterns, while the Rational Method is more effective in estimating surface discharge (Noor et al., 2021; Zhang et al., 2019). This method mostly used to calculate the maximum runoff volume of urban area (Wang and Wang, 2018).

The method works under some assumption such as; the rainfall intensity should uniformly distributed over time and space (Pilgrim and Cordery, 1993). Proper understanding and application of these methods aid in determining the size of sand traps and developing drainage systems that can prevent urban waterlogging (Campos et al., 2020).

This study aims to design sand traps to reduce sedimentation in drainage channels, enhance drainage capacity, and alleviate drainage congestion. Beyond Shahjalal Upashahar, the findings of this study would assist in effectively managing drainage systems facing severe sedimentation issues. This study would contribute to mitigating the impact of waterlogging in urban areas.

2. Materials and Methods

2.1. Study area

Shahjalal Upashahar is the most prominent urban area in Sylhet City. It is in the upstream of the Surma river basin in the northeastern part of Bangladesh, between 24°53’28” and 24°52’54" latitude, and 91°52’53” and 91°53’44” longitude. The Fig. 1. represented the study area.

Shahjalal Upashahar was assumed to be a catchment. Then it was split into five sub-catchments according to land use pattern, i.e., vegetative area, residential area, and street. The arial data was collected from National Housing Authority (NHA), Sylhet.

The catchment was divided in such a way that each catchment had a single outlet to the main drainage channel. The length and slope of each catchment were calculated by using ArcGIS. The drainage pattern of Shahjalal Upashahar was collected from the Sylhet City Corporation (SCC) to identify the high-risk congestion area in the drainage system. The local inquiry was also conducted to identify the high-risk congestion area.

2.2. Rainfall data collection

Daily rainfall data was collected for 24 years (2000- 2023) from the Bangladesh Meteorological Department (BMD). Then, the maximum rainfall per month was selected from the collected rainfall data. Furthermore, the yearly maximum 24-hour rainfall data was sorted for those years.

2.3. Estimation of t hour rainfall depth from rainfall depth per day

Rainfall depth of *t* hour was estimated from the rainfall depth of 24 hours. Depth was calculated for t minutes by using the following equation:

$$D_t = D_{24}\left(\frac{t}{24}\right)^{\frac{1}{3}} \tag{1}$$

Eq. 1 showed the calculation of *t* hour rainfall depth from one day rainfall depth. In this equation, D_t represented the rainfall depth of t-hour, and D_{24} was the rainfall depth over a 24-hour (Subramanya, 1994).

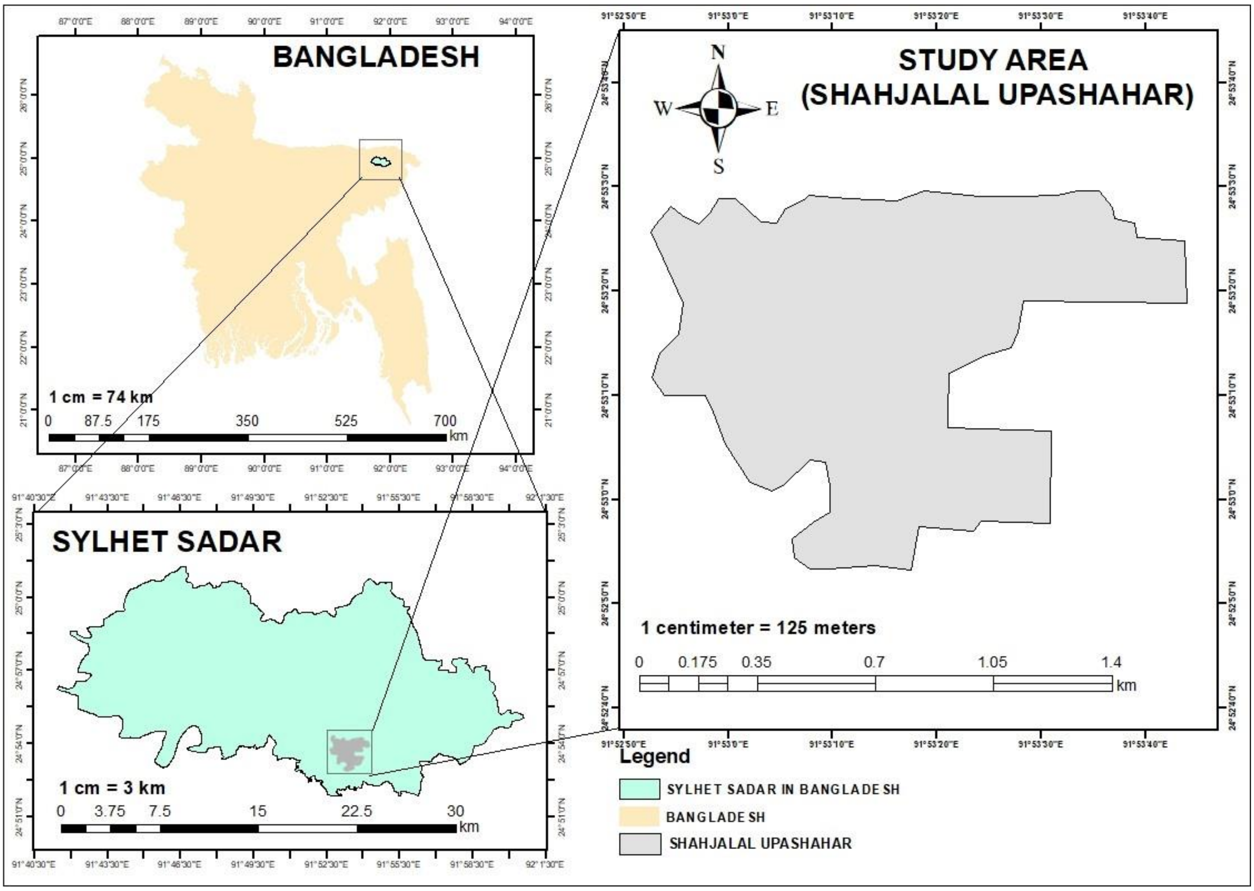

Fig. 1. Geographical map and location of Shahjalal Upashahar, Sylhet as the case study

2.4. Fitting the Gumbel distribution for t-hour rainfall depth

The rated t-hour rainfall depth was fitted using the Gumbel's function for the distribution method. Concerning Gumbel's function for distribution (1941):

$$Y_t = -\left[\ln.\ln\left(\frac{T}{T-1}\right)\right] \tag{2.a}$$

$$K = \frac{(y_t - y_n)}{S_n} \tag{2.b}$$

$$X_t = x + \partial_{n-1}k \tag{2.c}$$

Eq. 2.a showed the calculation of reduced variate for a return period *T*. In this equation Y_t denoted the reduced variate, and *T* was the return period.

Eq. 2.b. showed the calculation of frequency factors. In this equation, *K* denoted frequency factor, y_n represented reduced mean and S_n was the reduced standard deviation. Eq. 2.c. showed the calculation of rainfall depth for a return period. In this equation X_t represented the desired rainfall depth of t-hour for T-year return period, *X* was the mean of the t-hour rainfall depth and ∂_{n-1} denoted standard deviation of t-hour rainfall depth (Subramanya, 1994).

2.5. Calculation for t-year return period of t-minute rainfall depth

Depths of rainfall for varying lengths of time were calculated from depth & duration ratios for the same return period. The rainfall depths for 0.0833-hour, 0.167-hour, 0.25-hour, 0.5-hour, 1 hour, and 2 hours were calculated for various return periods (i.e.,25 years, 50 years, 75 years, and 100 years).

2.6. Assessing the intensity duration frequency (IDF) curve

Intensity of rainfall was estimated by dividing the rainfall depth for *t* minutes by the length of time. The IDF curve was constructed by placing the intensity along the *Y* axis and duration along the *X* axis.

2.7. Determination of volume of runoff

The rational method was used for calculating the volume of runoff. The intensity of rainfall was determined through the Intensity-Duration-Frequency curve for a time length which was equivalent to the time of concentration of a specific sub-catchment for a 100-year return period.

Peak runoff:

$$Q = \left(\frac{1}{360}\right) CIA \tag{3}$$

Eq. 3 showed the calculation of peak runoff discharge. In this equation Q denoted peak discharge (m^3s^{-1}) ,C was the coefficient of runoff , I was the intensity rainfall for a return period of T years (mm/hour) and A represented area of catchment (hectare) (Garg, 2009).

2.8. Evaluation of coefficient of runoff

Coefficient of runoff (C) depicted the interlaced impacts of different surface roughness, slope of the surface and intensity of rainfall (Subramanya, 1994). Due to non-homogeneous surface conditions, the total watershed was split into 5 sub-watersheds based on land use, such as residential, street, and vegetation areas. The respective runoff coefficients were collected from tables based on different land use pattern (Garg, 2009). The cumulative runoff coefficient was then determined by using the following equation:

$$C = \frac{\sum C_i A_i}{\sum A_n} \tag{4}$$

Eq. 4 showed the calculation of cumulative runoff coefficient. In this equation, C denoted the cumulative runoff coefficient, A_n was the area of the n^{th} sub-watershed (Garg, 2009).

2.9. Assessment of time of concentration

Time of concentration usually refers to the length of time required by a volume of runoff to reach from the most faraway location to the outlet of the drainage basin. The time of concentration for all sub-watersheds was evaluated to discover the desired intensity of rainfall for a specific return period.

$$T_c = \frac{0.01947\, L^{0.77}}{S^{0.385}} min \tag{5}$$

Eq. 5 showed the calculation of time of concentration of each respective sub-watershed. In this equation T_c was the Desired time of concentration of a sub-watershed area (min), L denoted the travel length by the runoff of a specific watershed area (m) and S represented the slope of the watershed area, (m/m) (Kirpich, 1940).

2.10. Determination of sand trap cross-section

The velocity of runoff for all sub-watershed areas was determined. The sand trap cross-section was determined by dividing the discharge of a specific sub-watershed area by the velocity of the runoff of this sub-watershed area.

$$A = \frac{Q}{V} \tag{6}$$

Eq. 6 showed the calculation of the cross-section area of sand trap. In this equation A was the desired cross section of sand trap, m^2, Q was the calculated peak discharge of sub catchment area, m^3s^{-1} and V was the velocity of flow m/s (Garg, 2009). From the calculated cross section, dimension of the rectangular sand trap was determined for each sub-watershed. For the Rectangular Cross-section of the Sand Trap:

$$A = W \times D \tag{7}$$

Eq. 7 showed the calculation of dimension for rectangular sand trap. In this equation W was the width of the sand trap (m) and D was the depth of the sand trap (m) (Garg, 2009).

2.11. Design of bar screen

The bar screen was designed based on

1. size of debris
2. The prevailing velocity of runoff
3. The materials used for the bar screen

3. Results and Discussion

Shahjalal Uposohor is situated between 24°53’28” and 24°52’54" latitude, and 91°52’53” and 91°53’44” longitude. In a previous study of Shahjalal Upashahar, they only focused on how to design a drainage system properly, but didn’t mention any way to increase the drainage capacity and reduce drainage congestion caused by sediment deposition in the drainage channel. Therefore, to cope up with this issue sand trap and bar screen mechanism was to be installed. For this purpose, the total watershed area was split into five sub-watershed areas based on land use pattern. The area of 1st, 2nd, 3rd, 4th, and 5th sub-catchments are 13000, 14423, 9788, 12427, and 13554 m^2 respectively.

3.1. Identification of high-risk congestion area

The drainage pattern map of Shahjalal Uposohor was collected from the Sylhet City Corporation. The high-risk congestion area in Fig. 2. was identified through local inquiry and questionnaire survey. The mapped zone showed narrow channel width and irregular flow path, confirming it as the most vulnerable location of waterlogging. These congestion-prone locations were frequently affected by waterlogging during high-intensity rainfall.

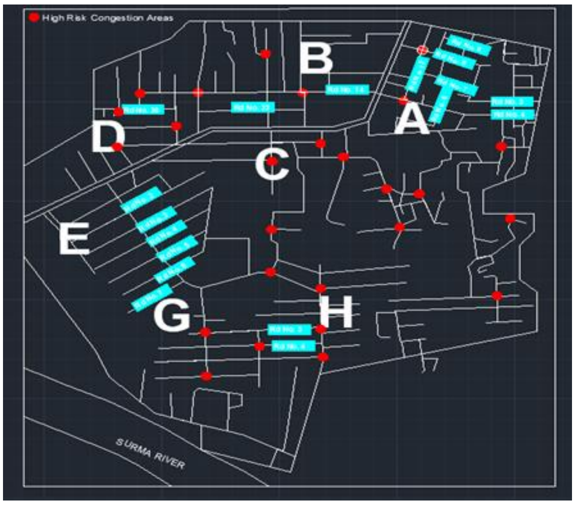

Fig. 2. High risk congestion area in Shahjalal Upashahar

3.2. Rainfall data plotting

Rainfall data were collected from the Bangladesh Meteorological Department. The maximum 24-hour rainfall per month was collected over 24 years (2000-2023). To assess the temporal variability and potential climate-induced changes in rainfall characteristics the long-term dataset was utilized. The change in rainfall pattern was evaluated. Fig. 3. showed how rainfall had fluctuated over the years in this region. The annual variation indicated that recent years experienced more intense rainfall events compared to earlier years and also highlighted the growing pressure on urban drainage channels in the region.

3.3. Estimation of rainfall depth for different return periods

Rainfall depths for durations of 5, 10, 15, 30, 60 and 120 minutes had been estimated in Table 1., based on the ratio of depth and duration for the same return period (Bell-1969).

The estimated rainfall depth demonstrated an increasing trend with both duration and return period. The rainfall at 100-year return period was the highest for all duration, confirming that extreme rainfall event produced significantly larger stormwater volume. These values were later used to calculate the rainfall intensities.

3.4. Curve of intensity duration frequency

The IDF curves were developed by plotting rainfall intensities against durations for different return periods. These curves showed that rainfall intensity decreased as the duration was increased. The 100-year return period line consistently produced the highest intensity values.

3.5. Determination of coefficient of runoff for each sub-watershed

Runoff coefficient is dependent on land use patterns i.e.; the vegetation area’s coefficient of runoff is not the same as for residential area. As the surface of catchment was non-homogeneous, the entire catchment was divided based on land use pattern of the study area. It included residential area, street and vegetation. Cumulative runoff coefficient was calculated in Table 2.

Runoff coefficients were determined based on land use type including residential area, street and vegetation cover. The coefficients of runoff for 1st, 2nd, 3rd, 4^{th,} and 5th sub-watersheds are 0.75, 0.95, 0.2, 0.75, and0.75, respectively. The street showed the highest coefficient (0.95), confirming that impervious surface produced more runoff, while vegetated area showed the lowest coefficient (0.2). The weighted average runoff coefficient for the watershed was found to be 0.71, indicating predominantly urban surface condition.

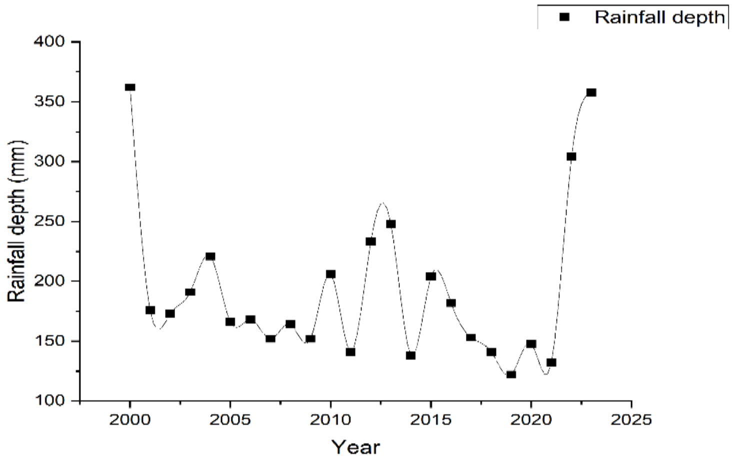

Fig. 3. Rainfall pattern

Table 1. Estimation of 5-, 10-, 15-, 30-, 60-, and 120-minutes rainfall depth for 25, 50, 75 and 100 years return period.

Depth of Rainfall (R)	25-year	50-year	75-year	100-year
P_{5min}	54.092	58.608	61.318	63.277
P_{10min}	67.683	73.314	76.692	79.134
P_{15min}	77.548	83.989	87.853	90.646
P_{30min}	97.709	105.82	110.688	114.206
P_{1hour}	123.098	133.321	139.455	143.888
P_{2hour}	155.094	167.974	175.702	181.288

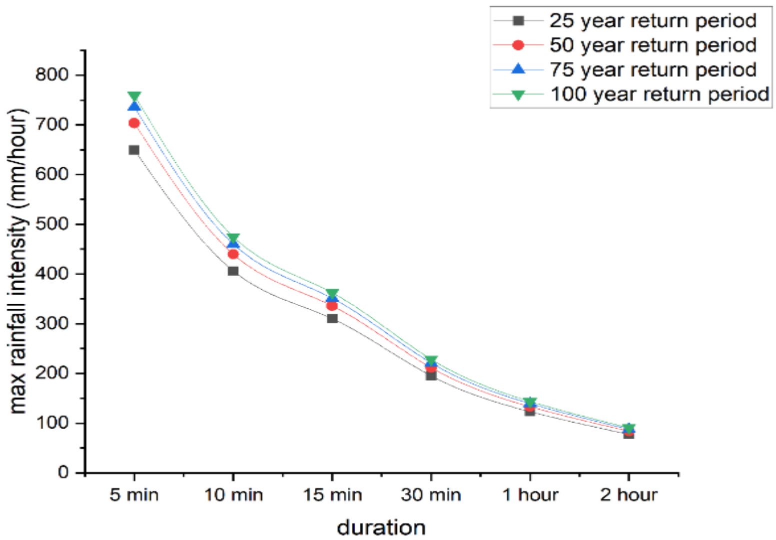

Fig. 4. Intensity-Duration-Frequency curve for different return periods

Table 2. Calculation of cumulative runoff coefficient

Sub Catchment	Land Use	Area, A_i (m²)	Runoff Coefficient, C_i	C_iA_i
C_1	Residential	13000	0.75	9750
C_2	Street	14423	0.95	13701.85
C_3	Vegetation	9788	0.2	1957.6
C_4	Residential	12427	0.75	9320.25
C_5	Residential	13554	0.75	10165.5
		$\sum A_i = 63192$		$\sum C_iA_i = 44895.2$
		$C = \sum C_iA_i / \sum A_i = 44895.2/63192 = 0.71$		

3.6. Calculation of time of concentration and flow velocity for areas of all sub-catchment

Length and slope for all sub-watershed areas were calculated using the ArcGIS. Time of concentration, t_c, was calculated based on the Kirpich formula (1940). Table 3. presented the calculation of time of concentration for each sub-watershed, while Table 4. shows the calculation for velocity of runoff.

Table 3. Calculation of time of concentration

Sub Watershed	Length	Slope	time of concentration (min)
C_1	536.63	0.0175	11.6855
C_2	561.66	0.0184	11.8715
C_3	459.36	0.0133	11.5223
C_4	593.21	0.0137	13.8707
C_5	512.57	0.0187	10.9955

The calculated value of time of concentration ranged between 10.9955 and 13.8707 min, depending on the slope and flow path. This result indicated that all catchment responded rapidly to rainfall events and delivered stormwater quickly to the drainage outlet.

Table 4. Calculation of flow velocity

Sub Watershed	Length	time of concentration (min)	Velocity (m/s)
C_1	536.63	11.6855	0.76
C_2	561.66	11.8715	0.79
C_3	459.36	11.5223	0.66
C_4	593.21	13.8707	0.71
C_5	512.57	10.9955	0.78

The flow velocity ranged from 0.66 m/s to 0.79 m/s across the sub-watershed. High velocity was observed where slope was stepper, confirming the strong relationship between gradient and flow speed. These values were used later to calculate the sand trap cross-sectional area.

3.7. Calculation of intensity of rainfall and highest discharge:

Intensity of rainfall for different return periods was calculated for a given time length from Fig.5. The time length was equivalent to the concentration time (t_c) of each respective sub-watershed.

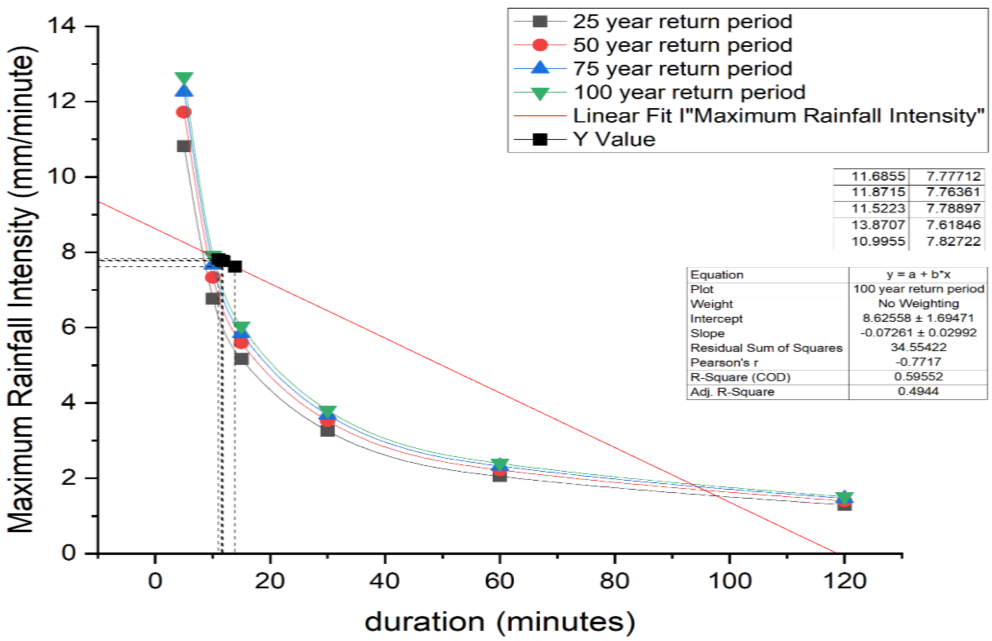

Fig.5. Calculation of Intensity of Rainfall from Time of Concentration

This figure represented the selection of rainfall intensity for each sub-watershed based on its time of concentration. The intensity value ranged from 457.107 to 469.633

mm/hour for 100-year return period. Design runoff volume was calculated using the rational equation (JICA-1991). The designed peak runoff was calculated for each sub-watershed in Table 5.

Design discharge: $Q = \left(\frac{1}{360}\right)CIA$

This table showed the final computed peak discharge for each sub-watershed ranging from 0.903 to 1.326 m^3/s. sub-watershed 2 generated the highest discharge due to its large impervious area and high rainfall intensity, while sub-watershed 3 produced the lowest runoff.

3.8. Design of sand trap and bar screen

3.8.1. Calculation of required cross-section of rectangular sand trap

Table 6. showed the calculated cross-sectional area and dimensions (width and depth) for each rectangular sand trap. The sand trap cross sectional area varied from 1.37 to 1.68 m^2 among sub-watersheds. The dimension result showed that each sub-watershed required different sized sand traps according to the discharge and flow velocity. Overall, all traps were adequately sized to settle the transported sediment.

3.8.2. Design of bar screen

Spacing of bars for fine debris was (6-20 mm) and for larger debris was (25-75 mm). Installation angle of bar screen was 45°- 60°. Allowable velocity of flow through bar screen was 0.25-0.65 m/s. Durable materials like stainless steel or galvanized was used to prevent corrosion.

The Fig. 6. illustrated the proposed placement of sand trap and bar screen within the drainage system. The bar screen to be positioned in front of sand trap. These arrangements ensure that the large debris to be filtered before trapping of the sediment.

Table 5. Calculation of peak discharge

Sub catchment	Coefficient of Runoff	Intensity of rainfall		Watershed area	Peak Discharge m3/sec
		mm/min	mm/hr		
C_1	0.75	7.712	466.272	1.30	1.263
C_2	0.95	7.6361	468.816	1.4423	1.784
C_3	0.2	7.7889	467.338	0.9788	0.254
C_4	0.75	7.6184	457.107	1.2427	1.183
C_5	0.75	7.8272	469.633	1.3554	1.326

Table 6. Calculation of dimensions of sand trap

Sub catchment	Peak discharge m^3/sec	Velocity m/sec	Cross -sectional area, m^2	Dimension of sand trap (m)	
				Depth(m)	Width(m)
C_1	1.263	0.76	1.66		1.66
C_2	1.784	0.79	2.26		2.26
C_3	0.254	0.66	0.38		0.38
C_4	1.183	0.71	1.67	1	1.67
C_5	1.326	0.78	1.70		1.70

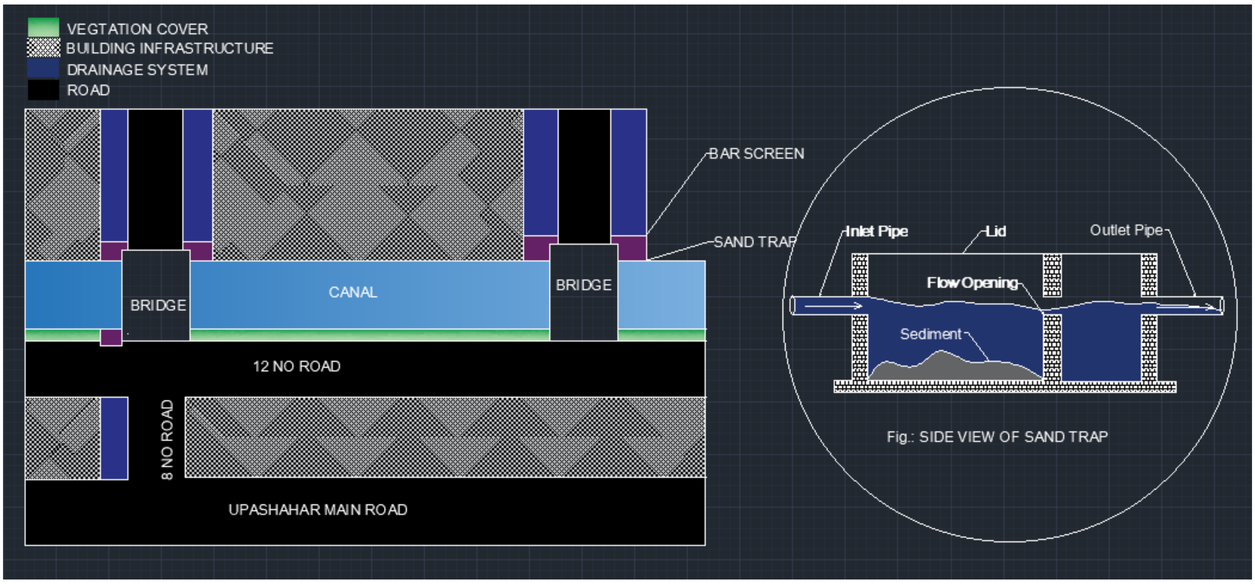

Fig. 6. Proposed Layout of Location of Sand Trap and Bar Screen in Drainage System

4. Conclusion

This study identified a high-risk congestion zone within the drainage channel, which was primarily caused by excessive sediment deposition. The results indicated that the reduced hydraulic capacity of the channel could be effectively improved through the installation of a properly designed sand trap and bar screen system.

Such a combined structure would not only mitigate sediment-induced congestion in the Shahjalal Upashahar drainage network but also serve as a practical solution for similar sediment-loaded drainage systems in comparable urban environments. Evidence from previous studies supported the effectiveness of sand traps in removing a substantial proportion of sediment before it entered downstream channels.

For instance, experimental investigations had reported sediment removal efficiencies ranging from 54% to 63%, while field trials in other regions had demonstrated removal rates of up to 70%. These findings reinforced the potential benefit of incorporating a sand trap, while the addition of a bar screen would further enhance system performance by preventing debris entry.

Overall, the findings of this study contributed to strengthening the resilience of urban drainage systems under increasing pressures from climate change and rapid urbanization. Implementing the recommended interventions can improve the operational efficiency and long-term capacity of the existing drainage network.

5. Acknowledgements

The authors thank the anonymous reviewers for providing constructive comments and suggestions.

6. Conflict of interest

No potential conflict of interest was reported by the authors.

7. References

Addison-Atkinson, W., Chen, A. S., Memon, F. A., Anta, J., Naves, J., & Cea, L. (2024). Investigation of uniform and graded sediment wash-off in an urban drainage system: Numerical model validation from a rainfall simulator in an experimental facility. *Journal of Hydrology,* 629, 130561. https://doi.org/10.1016/j.jhydrol.2023.130561

Ahmed, R., & Kim, I.-K. (2003). Patterns of Daily Rainfall in Bangladesh During the Summer Monsoon Season: Case Studies at Three Stations. *Physical Geography,* *24*(4), 295–318. https://doi.org/10.2747/0272-3646.24.4.295

Azir, A. I. (2025). Urban drainage challenges and mitigation approaches in Sylhet city. https://doi.org/10.30574/gscarr.2025.24.2.0251

Campos, J. N. B., Studart, T. M. d. C., Souza Filho, F. d. A. d., & Porto, V. C. (2020). On the rainfall intensity–duration–frequency curves, partial-area effect and the rational method: Theory and the engineering practice. *Water, 12*(10), 2730. https://doi.org/10.3390/w12102730

Chocat, B., Ashley, R., Marsalek, J., Matos, M., Rauch, W., Schilling, W., & Urbonas, B. (2007). Toward the sustainable management of urban storm-water. *Indoor and built environment, 16*(3), 273–285. https://doi.org/10.1177/1420326X07078854

Choudhury, S. A., Terao, T., Murata, F., & Hayashi, T. (2012). Seasonal variations of temperature and rainfall characteristics in the northeastern part of Bangladesh around Sylhet. J Agrofor Environ, 6(2), 81–88.

Cronshey, R. (1986). Urban hydrology for small watersheds. US Department of Agriculture, Soil Conservation Service, Engineering Division.

Dibaba, W. T. (2018). A review of sustainability of urban drainage system: traits and consequences. *Journal of Sedimentary Environments,* 131–137. https://doi.org/10.12957/jse.2018.37825

dos Santos, C. I., Carlotto, T., Steiner, L. V., & Chaffe, P. L. B. (2023). Development of the Synthetic Unit Hydrograph Tool–SUnHyT. *Applied Computing and Geosciences, 20*, 100138. https://doi.org/10.1016/j.acags.2023.100138

Garg, S. K. (2009). Irrigation Engineering And Hydraulic Structures. Khanna.

Gowdish, L., & Muñoz-Carpena, R. (2009). An improved Green–Ampt infiltration and redistribution method for uneven multistorm series. *Vadose Zone Journal, 8*(2), 470–479. https://doi.org/10.2136/vzj2008.0049

Hossain, M. A., Mahiuddin, S., Ahmad, A. U., & Monzurul Mamun, A. H. M. (2022). Causes and Effects of Water Logging in Dhaka City. In N. C. Jana & R. B. Singh (Eds.), Climate, Environment and Disaster in Developing Countries (pp. 153–171). Springer Nature Singapore. https://doi.org/10.1007/978-981-16-6966-8_8

Hua, J., Liang, Z., & Yu, Z. (2003). A modified rational formula for flood design in small basins 1. *JAWRA Journal of the American Water Resources Association, 39*(5), 1017–1025. https://doi.org/10.1111/j.1752-1688.2003.tb03689.x

Huong, H. T. L., & Pathirana, A. (2013). Urbanization and climate change impacts on future urban flooding in Can Tho city, Vietnam. *Hydrology and Earth System Sciences, 17*(1), 379–394. https://doi.org/10.5194/hess-17-379-2013

Islam, N., & Rahman, M. A. (2022). Assessment of Drainage Congestion at Sylhet City of Bangladesh and Development of Stormwater Drainage Masterplan Using GeoSWMM Model. Authorea Preprints. https://doi.org/10.1002/essoar.10511683.1

Jain, M., Tripathi, L., Bhambota, P., & Dangi, A. (2025). Comparative Review of Hydrological Models for Runoff Estimation: A Focus on SCS-CN, TOPMODEL, and VIC Approaches– A Review. *International Journal of Research and Review in Applied Science, Humanities, and Technology,* 121–135. https://doi.org/10.71143/z9v3aj80

Kirpich, Z. (1940). Time of concentration of small agricultural watersheds. *Civil engineering, 10*(6), 362.

Lu, Q.-O., Bahramloo, R., Rodrigo-Comino, J., Wang, J., Talebi, A., Tran, Q. T. P., Ghahramani, A., & Sepehri, M. (2025). Evaluating the impact of roof rainwater harvesting on hydrological connectivity and urban flood mitigation. *Results in Engineering, 25*, 104022. https://doi.org/10.1016/j.rineng.2025.104022

Miller, J. E. (1984). Basic concepts of kinematic-wave models [Report](1302). (Professional Paper, Issue. U. S. G. Survey. https://pubs.usgs.gov/publication/pp1302

Noor, M., Ismail, T., Shahid, S., Asaduzzaman, M., & Dewan, A. (2021). Evaluating intensity-duration-frequency (IDF) curves of satellite-based precipitation datasets in Peninsular Malaysia. *Atmospheric Research, 248*, 105203. https://doi.org/10.1016/j.atmosres.2020.105203

Phanuwan, C., Takizawa, S., Oguma, K., Katayama, H., Yunika, A., & Ohgaki, S. (2006). Monitoring of human enteric viruses and coliform bacteria in waters after urban flood in Jakarta, Indonesia. *Water Science and Technology, 54*(3), 203–210. https://doi.org/10.2166/wst.2006.470

Pilgrim, D. H., & Cordery, I. (1993). Chapter 9: Flood Runoff. Handbook of Hydrology. McGraw-Hill, New York, USA.

Roy, E., Rahman, M. S., Nisha, N. S., & Majumder, A. (2022). *Water vulnerability and sustainability scenario of a typical populus city of least developed country*. Proceedings of the 5th International Conference on Civil Engineering for Sustainable Development,

Sarker, A. A., & Rashid, A. M. (2013). Landslide and flashflood in Bangladesh. In Disaster risk reduction approaches in Bangladesh (pp. 165–189). Springer. https://doi.org/10.1007/978-4-431-54252-0_8

Subramanya, K. (1994). Engineering Hydrology. McGraw-Hill.

Ten Veldhuis, J., & Clemens, F. (2010). Microbial risks associated with exposure to pathogens in contaminated urban flood water. *Water research, 44*(9), 2910–2918. https://doi.org/10.1016/j.watres.2010.02.009

Thodesen, B., Time, B., & Kvande, T. (2022). Sustainable Urban Drainage Systems: Themes of Public Perception—A Case Study. *Land, 11*(4), 589. https://doi.org/10.3390/land11040589

Vairavamoorthy, K., Gorantiwar, S. D., & Pathirana, A. (2008). Managing urban water supplies in developing countries–Climate change and water scarcity scenarios. P*hysics and Chemistry of the Earth, Parts A/B/C, 33*(5), 330–339. https://doi.org/10.1016/j.pce.2008.02.008

Wang, S., & Wang, H. (2018). Extending the Rational Method for assessing and developing sustainable urban drainage systems. *Water research, 144*, 112–125. https://doi.org/10.1016/j.watres.2018.07.022

Zhang, W.-b., Rao, W.-b., Li, L., Liu, Y., Wang, S., Jin, K., & Zheng, F.-w. (2019). Compressibility and hydraulic conductivity of sand-attapulgite cut-off wall backfills. *Journal of Zhejiang University-Science A, 20*(3), 218–228. https://doi.org/10.1631/jzus.A1800548